Adsorption 11: 21–28, 2005

Nanospace Molecular Science and Adsorption

KATSUMI KANEKO*, TOMONORI OHBA AND TAKAHIRO OHKUBO
Department of Chemistry, Faculty of Science, 1-33 Yayoi, Inage, Chiba 263-8522, Japan
kaneko@pchem2.s.chiba-u.ac.jp

SHIGENORI UTSUMI
Center for Frontier Electronics and Photonics,Chiba University, 1-33 Yayoi, Inage, Chiba 263-8522, Japan

HIRONOBU KANOH
Department of Chemistry, Faculty of Science, 1-33 Yayoi, Inage, Chiba 263-8522, Japan; Center for Frontier Electronics and Photonics, Chiba University, 1-33 Yayoi, Inage, Chiba 263-8522, Japan

MASAKO YUDASAKA
JST/SORST, NEC Corporation, 34 Miyukigaoka, Tsukuba 305-8501, Japan

SUMIO IIJIMA
JST/SORST, NEC Corporation, 34 Miyukigaoka, Tsukuba 305-8501, Japan; Department of Physics, Meijo University, 1-501 Shiogamaguchi, Tenpaku, Nagoya 468-8502, Japan

Abstract. The relationships between the enhanced interaction potential and intensive confinement effect of slit-shaped and cylindrical nanospaces are shown. The structures of water molecules and aqueous ions confined in nanospaces of activated carbon fiber (ACF) and single wall carbon nanohorn (SWNH)s were studied by adsorption, in situ small angle X-ray scattering(SAXS), GCMC simulation, and EXAFS spectroscopy. Water molecules are associated with each other to form the clusters, being stabilized in the carbon nanospaces. This stabilization mechanism of water in carbon nanospaces were evidenced by the interaction potential calculation, GCMC simulation, and the density fluctuation analysis of in situ SAXS. The Ornstein-Zernike analysis of in situ SAXS profiles lead to the conclusion that the critical size of water clusters for predominant water adsorption in hydrophobic carbon nanospaces is about 0.5 nm corresponding to the octomer to decamer. The adsorption hysteresis of water adsorption isotherm of nanoporous carbon was interpreted by the cluster growth, which is confirmed by the density fluctuation analysis. The Rb and Br ions confined in the carbon nanospaces were examined by EXAFS spectroscopy. The remarkable decreases in the hydration number and the water-Rb ion distance of the solution confined in the nanospaces were observed. In particular, the hydration number of the Rb ion in the nanospaces of SWNH is less than 3, being much smaller than the hydration number (6) of the bulk solution. The electrical double layer structure in the nanospaces should be quite different from that in the bulk solution.

Keywords: adsorption, activated carbon fiber, single wall carbon nanohorn, nanoconfinement, water, nanosolution

*To whom correspondence should be addressed.

1. Introduction

Human is in the critical situation for harmonization with earth environments. Hence science has a great charge for such a social demand. Adsorption science is one of key sciences, which is deeply associated with energy, resources, environmental, and medical technologies. Therefore, we need to continue to study adsorption science with the relevance to future contribution to the preservation of earth environments. At the same time, we must show new progresses in adsorption area which can affect intensively the surrounding academic regions. One possible approach is on solid nanospace chemistry, which can offer a wide basis for molecular science, catalysis science, interface chemistry, solid state chemistry, electrochemistry, and solution chemistry.

Solid nanospaces have an enhanced molecular field. The interaction profile between the nanopore and a molecule can distinguish monolayer process from confined process in the restricted space; the monolayer process can be regarded as the surface process, whereas the confined process cannot be described by the ordinary surface process. The typical confined processes of molecules can be observed in nanopores whose pore width is less than the double layer thickness of the adsorbate molecule. Such a narrow nanopore must be named nanospace. The strict nanospaces are limited to nanopores whose width is less than bilayer thickness of the molecule. However, the residual space between the monolayers on the pore walls can also offer an enhanced interaction potential for molecules (Ohba et al., 2000) and thereby the term of solid nanospaces has been used even for pores whose pore width is larger than the bilayer thickness of the molecule. Kaneko et al. have been studying molecular assemblies in carbon nanopores, showing that molecules form a self-organized molecular assembly depending on the molecule-pore wall interaction (Kaneko, 2000). Accordingly, if we can understand and control the unique nature of nanospaces, we can develop new chemistry and chemical engineering. For example, confinement of supercritical gases such as methane and hydrogen is deeply associated with clean energy technology (Menon and Komarneni, 1998; Ding et al., 2001). The confinement of molecules often induces high pressure reaction, which is named quasi-high pressure effect (Imai et al., 1991; Nishi et al., 1997). At the same time, the confinement of molecules in the nanospaces leads to stabilization of unstable clusters or phase (Kaneko et al., 1987) water in carbon nanospaces has a solid-like structure (Iiyama et al., 1995, 1997), while ethanol molecules form a highly oriented structure (Ohkubo et al., 1999). The freezing temperature of organic solvents is elevated in carbon nanospaces (Kaneko et al., 1999; Radhakrishnan et al., 1999). Thus, nanospace molecular science which is a new science born from adsorption area has a hopeful guide line for new technologies.

In this paper, recent progresses on molecules and ions confined in nanospaces of activated carbon fiber (ACF) and single wall carbon nanohorn (SWNH) are reviewed.

2. Enhanced Pore Potential Fields

The interaction potential profile of a molecule with the pore can be obtained using Lennard-Jones(LJ) pair potential-based function for slit and cylindrical pores. In particular, well-known structure-less potential functions have been available for calculation of the interaction between a molecule and the slit or cylindrical carbon pore. In the case of the graphite slit pore which is a model for activated carbon.

The steele 10-4-3 potential function $\Phi(z)$ gives the interaction potential energy of a molecule distant from the surface by z (vertical distance). Hence, the interaction potential $\Phi(z)_p$ of a molecule with two graphite slabs is given by,

$$\Phi(z)_{\mathrm{p}} = \Phi(z) + \Phi(\mathrm{H}\text{-}z) \tag{1}$$

Here H is the inter-graphite surface distance, which is associated with the effective pore width w (being the experimental pore width) using $w = \mathrm{H} - 0.24$ (nm) for a N_2 molecule (Kaneko et al., 1994).

Figure 1 shows the interaction potential profiles for N_2-graphite slit pore system as a function of w. The double potential minima disappear for pores of $w \leqq 0.6$ nm. Even the pore of $w = 0.7$ nm has no distinct double minima. Therefore, the pores whose width is less than about 0.6 nm can offer molecular processes not including an explicit monolayer process. Even the pores whose width is larger than 0.6 nm can also offer a special potential filed, because the preformed monolayer on the pore wall can provide a single potential minima. Of course, the above critical pore width depends on the adsorbate molecule and the solid surface.

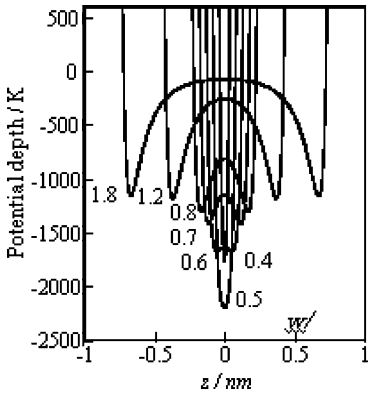

Figure 1. Interaction potential profiles of N_2 with graphite slit pore as a function of effective pore width nm.

The potential profiles for a molecule in the cylindrical pore and at the external wall surface of the cylindrical pore of structure-less single graphene sheet, being the model of single wall carbon nanotube (SWNT) are obtained using the established potential function (Tanaka et al., in press). The interaction potential profiles for N_2 in the pore of SWNT as a function of $w$give tendency similar to those for N_2 in the slit pore, although the potential is much deeper for the same w value; the potential of SWNT is deeper than that of the slit pore for $w = 0.7$ nm by about 700 K. In the case of single SWNT particle, the potential depth for an internal molecule is much deeper than that for an external molecule; for example the potential depth difference is about 1000 K for $w = 2.5$ nm. However, SWNTs always form the bundle structure. Therefore we must take into account the interstitial pores among the SWNT bundle. The interstitial pores of one-dimensionality give deeper interaction potential than the internal tube space, because the interstitial pore space is surrounded by three or four convex SWNT walls.

3. Control of Open Nanoporosity of Single Wall Carbon Nanohorns

Iijima clearly showed the structural uniqueness of SWNT in 1991 (Iijima, 1991) and a variety of studies on SWNT have been carried out (Dresselhaus et al., 1996; Saito et al., 1998; Tanaka et al., 1999). SWNT has been produced with metallic catalysts and removal of those catalysts is quite difficult (Yang, 1992); sufficient amounts of highly pure SWNT are not available for adsorption studies. Accordingly, reliable chemical studies on SWNT are less advanced compared with physical ones. SWNH was found in the arc-evaporated carbon products with TEM in 1994 (Harris et al., 1994); it was not available for other fundamental studies. Iijima et al. succeeded to produce sufficient amount of highly pure SWNH by laser ablation of pure graphite without any metal catalysts (Iijima et al., 1999). An individual SWNH particle is composed of a graphene sheet shaped into a tube with conical cap. The mean diameter and length are 2–4 nm and 40–50 nm, respectively. SWNH particles are associated with each other to form a radial assembly with a spherical form having a diameter of 80–100 nm. The recent X-ray diffraction and N_2 adsorption studies on the SWNH assemblies showed the presence of a partially bundled structure which provides quasi-one dimensional nanospaces of the interstitial pores like SWNT (Ohba et al., 2001, to be submitted), XPS and heat of wetting experiments showed almost absence of surface oxygen on SWNH (Bekyarova et al., 2002).

In this work, we oxidized SWNH at 663 and 823 K under an oxygen atmosphere at the flow rate of 10 ml min^{-1} for 10 min. The N_2 adsorption isotherm of oxidized SWNH samples was measured at 77 K. The SWNH samples were analyzed with DTA and TG system under an oxygen atmosphere over the temperature range of 373 to 1073 K. Figure 2 shows DTA charts

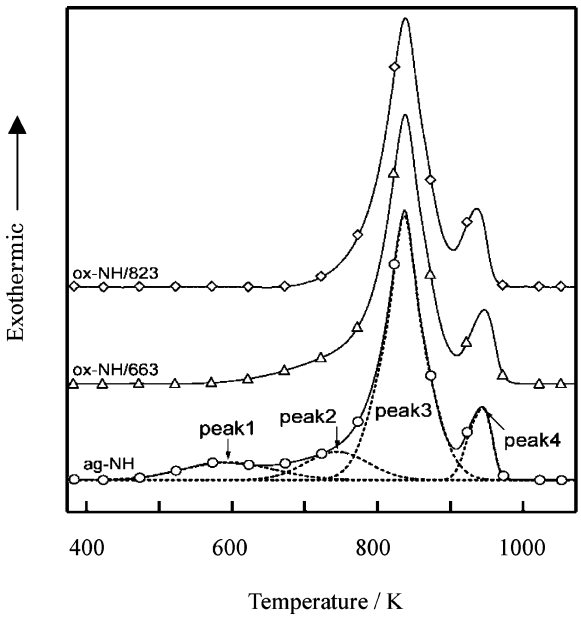

Figure 2. DTA charts of SWNH oxidized at different temperatures. ○: close SWNH, △: SWNH oxidized at 663 K, ◇: SWNH oxidized at 823 K.

of as-received SWNH and SWNH oxidized at 663 and 823 K. The DTA chart of the as-received SWNH has four peaks at 594 K (peak 1), 744 K (peak 2), 837 K (peak 3), and 944 K (peak 4). The peak 1 of SWNH oxidized at 663 K and 823 K disappears. The DTA chart of SWNH oxidized at 823 K has predominat peaks 3 and 4; the peak 2 almost disappears. The peak 1 and peak 2 can be assigned to oxidation of amorphous carbon and corn parts of non-hexagons, respectively. The examination of these treated samples with Raman spectroscopy and X-ray diffraction gave the conclusion that the peak 3 and peak 4 stem from the oxidation of tubular carbons and graphite core, respectively. SWNH contains amorphous carbon (2 wt.%) and graphite core (12 wt.%), although SWNH is chemically pure. As the specific surface area of the graphite core is nil, the contribution to adsorption can be neglected. We did not correct the contribution by amorphous carbon to gas adsorption on SWNH samples, because SWNH itself has nanopores of high surface area.

4. Organization of Molecules and Ions in Graphitic Nanospaces

These authors have studied the structures of molecules confined in graphitic slit nanospaces of activated carbon fiber (ACF) for CCl_4, Xe, N_2, O_2, NO, SO_2, He, water, and alcohol. CCl_4 molecules are nonpolar and roughly spherical and form a specific assembly structure of the low temperature solid phase of bulk CCl_4 in the carbon nanospaces at 303 K (Iiyama et al., 1997; Suzuki et al., 1999). Even Xe forms clusters of a variety of association number in the nanospaces at 303 K (Aoshima et al., 1999). O_2 forms inherent spin clusters, which are affected by coexistent CO_2 (Tohdoh and Kaneko, 2001). NO molecules are dimerized in the nanospaces even at supercritical conditions (Kaneko et al., 1987). Water molecules in the carbon nanospaces provide an ordered structure similar to solid even at 303 K and the confined water does not freeze even at 143 K (Iiyama et al., 2001). The adsorbed density of C_2H_5OH in the slit-shaped nanospaces is close to the solid density of C_2H_5OH at 303 K; the X-ray diffraction study provides that C_2H_5OH molecules form a highly oriented structure along the pore wall. The orientation of alcohol molecules of CH_3OH, C_2H_5 OH, and C_3H_7OH in the slit-shaped pores depends on the chain length (Ohkubo et al., 2001).

The authors have started the studies on nanospace molecular science on SWNH which has well-characterized nanospaces than ACF. Recent studies showed that the adsorbed H_2 density in the nanospaces of SWNH at 20 K is close to the bulk solid density and quantum effect is quite essential in the nanospaces (Tanaka et al., in press), and quantum molecular sieving effect in H_2 and D_2 adsorption on SWNH is remarkable even at 77 K (Tanaka et al., to be submitted). The unique adsorption mechanism of supercritical H_2 in the nanospaces of SWNH is observed (Murata et al., 2002).

In this article, recent results on cluster-associated water adsorption and ionic solution confined in nanospaces of ACF and SWNH are described.

4.1. Cluster-Aided Water Adsorption in Hydrophobic Nanospaces

A water drop is stable on the surface of the highly oriented pyrolytic graphite, indicating that carbon without surface functional groups has a typical hydrophobicity. However, water vapor is predominantly adsorbed on activated carbon of a few surface functional groups. The maximum adsorption volume of water vapor on activated carbon is almost equal to the micropore volume, assuming that the density of adsorbed water is the bulk liquid density. The adsorption on activated carbon of surface functional groups begins from the low relative pressure *P/P*o (Kaneko et al., 1989, 1999; Mowia et al., 2003), where as the predominant adsorption starts near $P/Po = 0.5$ for activated carbon free of surface functional groups (Ohba et al., in press; Kimura et al.).

The established mechanism of water adsorption on activated carbon comes from the presence of surface functional groups; water molecules are adsorbed on the surface oxygen sites of carbon pores through hydrogen bonding, forming the clusters of adsorbed molecules (Dubinin et al., 1955; Mowia et al., 2003). However, water vapor can be adsorbed on activated carbon treated at high temperature in a hydrogen atmosphere. Also, water vapor cannot be adsorbed in mesopores at P/Po corresponding to the pore width, but only in micropores for activated carbon aerogels (Hanzawa and Kaneko, 1997). Consequently, Kaneko et al. proposed the hypothetical stabilization mechanism of water clusters in carbon micropores (Kaneko et al., 1999). Recently, Ohba et al. calculated the total interaction potential profiles of a cluster with carbon slit pore using TIP5P and steele 10-4-3 function (Ohba et al., 2004).

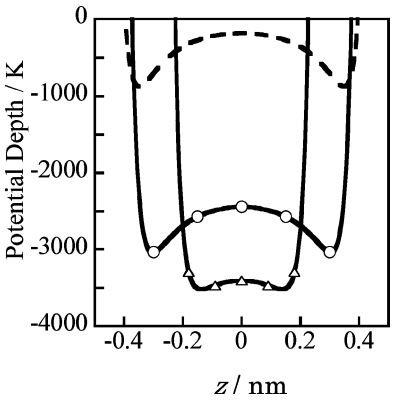

Figure 3. Total potential profiles of a water molecule of the cluster with graphite slit pore. ○: Tetramer, △: Octamer, - - - -: Monomer.

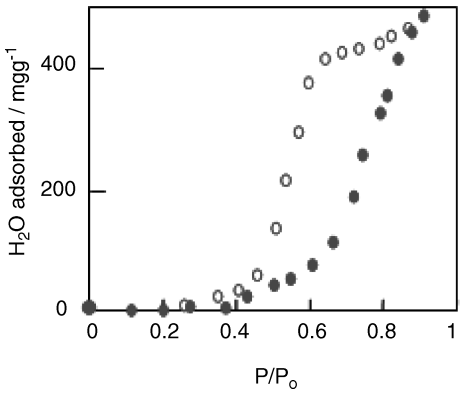

Figure 4. Adsorption isotherm of water on open SWNH at 303 K; ●: Adsorption and ○: Desorption.

Figure 3 shows the total potential profiles for a water molecule of the tetramer and octamer with the graphitic slit space of $w = 1.1$ nm together with the interaction potential profile of a single water molecule. As the tetramer and octomer are larger than the single molecule, the position of the potential minimum shifts from the monolayer position for the single molecule near the center of the slit space. The water molecules get a great stabilization energy through cluster formation. That is, water molecules gain an apparent hydrophobicity through cluster formation; the interaction energy of the octomer is more than 3500 K.

In situ small angle X-ray scattering (SAXS) provides the correlation length and the density fluctuation with Ornstein-Zernike analysis (Iiyama et al., 2001, 2004). The in situ SAXS measurement of water confined in nanospaces of ACF at different fractional filling leads to the presence of the critical correlation length, which is evaluated to be the unit cluster size of 0.5 nm. The size of the octomer to decamer is about 0.5 nm in diameter. Accordingly, the critical unit size of water clusters should be the octomer to decamer. At the same time, GCMC simulation of water adsorption in a graphite slit pore at 303 K gives an almost vertical adsorption isotherm near $P/P\mathrm{o} = 0.5$, agreeing with the observed desorption isotherm on ACF. The snapshot of water molecules in the nanospace from the GCMC simulation shows the growth of water clusters along the vertical adsorption. Thus, water adsorption mechanism on carbon nanospaces can be understood in terms of the formation of water nanoclusters and their growth.

Similar approaches were carried out for water adsorption on SWNH assemblies. Water vapor can be adsorbed on SWNH assemblies irrespective of almost nil of surface functional groups (Bekyarova et al., 2002). Figure 4 shows water adsorption isotherm of open SWNH at 303 K. The open SWNH was obtained by oxidation at 823 K. Adsorption on open SWNH includes adsorption in interstitial nanospaces and intratube nanospaces. However, adsorption amount in interstitial nanospaces is 20% of that in the intratube nanospaces; the adsorption isotherm in Fig. 4 can be regarded as adsorption in intratube nanospaces approximately. There is a predominant adsorption increase above $P/P\mathrm{o} = 0.7$, accompanying with an explicit adsorption hysteresis. As the pore size of SWNH assemblies distributes from subnanometer to nanometer due to the distribution of the tube diameter. The small clusters are isolated each other and they grow gradually until about $P/P\mathrm{o} = 0.7$, merging to provide the abrupt adsorption increase.

The water adsorption in intratube nanospaces of open SWNH was examined with in situ SAXS, leading to the relationship between the density fluctuation and fractional filling of the nanospaces with molecules. The density fluctuation increases up to 1.6 around 0.45 of fractional filling and then decreases to 1.2 at the perfect filling on the course of adsorption process. On the course of desorption, the density fluctuation has almost constant value of 1.2 until 0.3 of fractional filling and then reduces to 1 at zero of the fractional filling. An alternately arranged cluster model gives 1.6 of the density fluctuation, whereas the monolayer adsorbed model provides 1.0 of the density fluctuation. This simple geometrical distribution of clusters or molecules is briefly close to the snapshots obtained by the GCMC simulation. Therefore, water molecules form the clusters, which are isolated with each other at the half

fractional filling; with increasing the fractional filling, the clusters merge each other to form uniform adsorbed layer in the nanospaces for adsorption process. On the other hand, water molecules are detached from the uniform adsorbed layer through the monolayer structure for desorption.

4.2. Partially Dehydrated Structure of Ions Adsorbed in Carbon Nanospaces

Adsorption of heavy metal ions is one of important research subjects in adsorption science. However, almost all adsorption studies just measure the adsorption isotherm of metal ions on the target materials as a function of pH. In adsorption from solution, competitive adsorption of solvent molecules and solvent-adsorbate interaction must be taken into account. A specific approach to elucidate adsorption from solution must be introduced. Although spectroscopic and nanoscopic techniques have been applied to liquid phase adsorption on the flat solid surfaces, liquid phase adsorption in nanopores still wait for pioneering researches using an appropriate technique. Recently, we have an intensive demand for fundamental study on supercapacitors which are hopeful clean energy storage devices for automobiles. The electrolytic solution is introduced in the nanopores of conductive materials (nanoporous carbons in almost cases), providing the superhigh capacitance due to the electric double layer on the electrodes of the great surface area (Oren and Soffer, 1985; Tanahashi et al., 1990). However, the electric double layer concept stems from the macroscopic structure and we do not understand the electric double layer of "electrolytic solution" confined in the nanopores. Development of a higher performance-supercapacitor device needs better understanding of "electric double layer structure" of ions in the nanospaces. The structural studies on electrolytic solution confined in solid nanospaces have been requested. Here, we name the confined solution as nanosolution (NSN).

We have tried to determine the hydration structure of ions in the carbon nanospaces using X-ray absorption spectroscopy. In particular, EXAFS provides the local structure around the target ion. The EXAFS was applied to the model NSN of RbBr in nanospaces of ACF (Ohkubo et al., 2002, 2003) and SWNH, because both ions have larger atomic numbers, leading to reliable data of X-ray absorption. Here, ionic radii of Rb^+ and Br^- are 0.149 and 0.195 nm, respectively. We used ACFs of which average pore width are 0.7 nm and 1.1 nm, respectively. Also close and open SWNH samples were used. The close SWNH has the quasi one-dimensional interstitial nanospaces of which pore width is 0.6 nm. The carbon sample was dipped in 1 M solution and dried. Water vapor was adsorbed on the RbBr dispersed carbon samples, providing RbBr nanosolution in the nanospaces. The high dispersion state of RbBr on carbon samples was confirmed by use of EXAFS in advance. EXAFS of the Rb K-edge (15.2036 Kev) and Br K-edge (13.4799 Kev) were measured using a specially designed sample cell with Mylar film windows at KEK, Tsukuba.

Figure 5 shows the radial structure functions of bulk solution (IM) and NSN (IM) in nanospaces of open and close SWNH samples. The difference in these radial structure functions must be elucidated by the established fitting procedure. The radical structure functions of confined solutions around Rb and Br ions after the least square fit of Fourier Filtered EXAFS spectra were determined, leading to the local structure parameters. The analysis of the EXAFS oscillation around a Br ion could not provide highly reliable results and

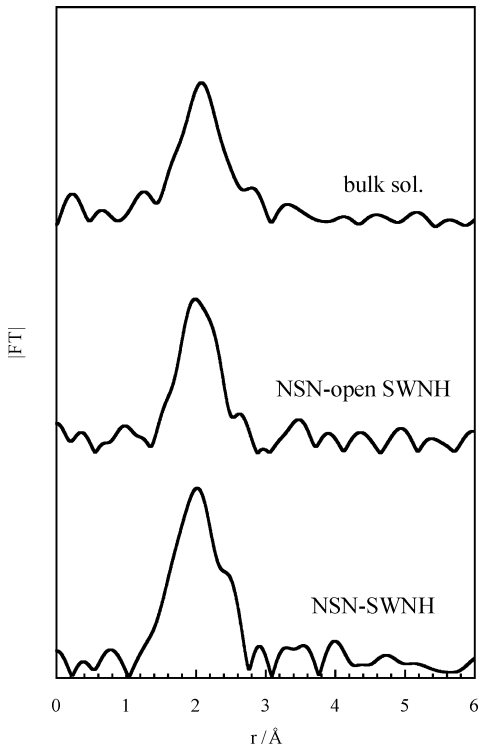

Figure 5. Radial structure functions around a Rb ion for nanosolution prepared in nanospaces of SWNHs.

Table 1. Hydration number of the Rb ion and water-Rb ion distance.

Solution	r(Rb—O)/nm	N(Rb—O)
NSN of ACF-1.1 nm	0.284	5.3
NSN of ACF-0.7 nm	0.285	3.9
NSN of close SWNH	0.290	2.6
NSN of open SWNH	0.293	2.6
Bulk solution	0.320	6.0

thereby local structure parameters around a Rb ion will be given below.

Table 1 shows structural parameters of Rb-O distance r(Rb-O)(O denotes an oxygen atom of a water molecule) and coordination number around a Rb ion N(Rb-O) (hydration number). The Rb-O distance of confined solution is smaller than that bulk solution by more than 0.03 nm. Hence, the first hydration shell of the Rb ion must shrink in the nanospaces. The difference in the Rb-O distance for ACF and SWNH is not so great. A remarkable decrease in the hydration number of confined solution is observed. As the hydration number in the bulk solution is not uniquely established, we assumed six of the hydration number of the bulk solution.

The hydration number of a Rb ion confined in the slit nanospace of $w = 0.7$ nm is only 3.9, being much smaller than the bulk value. The slit nanospace of $w = 1.1$ nm gives 5.3 of the hydration number. The hydration number of the Rb ion in the interstitial and intratube nanospaces of SWNH assembly is only 2.6, suggesting the possibility of dehydration along the one-dimensional space in part. Both of r(Rb-O) and N(Rb-O) evidence that local structures around the Rb ion in the nanospaces are completely different from those in the bulk phase. Therefore, we cannot extend the electrical double layer concept in the bulk phase to solution confined in the nanospaces; a more dense ionic state is realized in the nanospaces. The EXAFS gives another structural parameter, the Debye-Warrer(DW) factor which is associated with thermal fluctuation. A smaller DW value indicates presence of a more organized structure around the target atom. The DW factors of confined solution are smaller than that of the bulk solution. In particular, the DW factor of solution confined in the nanospaces of SWNH was much less than that of the bulk value. Therefore, water molecules around hydrated ions should form a highly ordered structure, which should be solid like (Iiyama et al., 1985). We have extended this study to transition metal ion solution.

Acknowledgments

This work was funded by the Grant-in-Aid for Scientific Research S(15101003) from Japanese Government and in part by the Nanocarbon project from the New Energy and Industrial Technology Development Organization of Japan. T. Ohkubo and T. Ohba were supported by Research Fellowship of the Japan Society for the Promotion of Science for Young Scientists.

References

Aoshima, M. et al., "Molecular Association-Mediated Micropore Filling of Supercritical Xe in a Grapite Slit Pore by Grand Canonical Monte Carlo simulation," *Chem. Phys. Lett*., **310**, 1–7 (1999).

Bekyarova, E. et al., "Cluster-Mediated Filling of Water Vapor in Intratube and Interstitial Nanospaces of Single Wall Carbon Nanohorns," *Chem. Phys. Lett*., **366**, 461–468 (2002).

Ding, R.G. et al., "Recent Advances in the Preparation and Utilization of Carbon Nanotubes for Hydrogen Storage," *J. Nanosci. Nanotech.*, **1**, 7–29 (2001).

Dresselhaus, M.S. et al., *Science of Fullerenes and Carbon Nanotubes*, Academic Press, New York 1996.

Dubinin, M.M. et al., "The Sorption of Water Vapor by Activated Carbon," *J. Chem. Soc.*, **1955**, 1760–1766.

Hanzawa, Y. and K. Kaneko, "Lack of a Predominant Adsorption of Water Vapor on Carbon Mesopores," *Langmuir*, **13**, 5802–5804 (1997).

Harris, P.J.F. et al., "High-Resolution Electron Microscopy Studies of a Microporous Carbon Produced by Arc-Evaporation," *J. Chem. Soc. Faraday Trans.*, **90**, 2799–2802 (1994).

Iijima, S., "Helical Microtubules of Graphitic Carbon," *Nature*, **354**, 56–58 (1991).

Iijima et al., "Nanoaggregates of Single Walled Graphitic Carbon Nanohorns," *Chem. Phys. Lett.*, **309**, 165–170 (1999).

Iiyama et al., "An Ordered Water Molecular Assembly Structure in a Slit Shaped Carbon Nanospaces," *J. Phys. Chem*., **99**, 10078–10079 (1995).

Iiyama et al. "Study of the Structure of a Water Molecular Assembly in a Hydrophobic Nanospaces at Low Temperature With in Situ X-ray Diffraction," *Chem. Phys. Lett.*, **274**, 152–158 (1997).

Iiyama, T. et al., "Molecular Assembly Atructure of CCl_4 in Graphitic Nanospaces," *J. Phys. Chem. B*, **101**, 3037–3042 (1997).

Iiyama, T. et al., "Structural Mechanism of Water Adsorption with in Situ Small Angle X-ray Scattering," *Chem. Phys. Lett*., **331**, 359–364 (2001).

Iiyama, et al., "In Situ Small-Angle X-ray Scattering Study of Cluster Formation in Carbon Micropores," *Coll. Surf. A*, **241**, 207–213 (2004).

Imai, J. et al., "Reaction of Dimerized NOx ($x = 1$ or 2) with SO_2 in a Restricted Slit-Shaped Micropore Space," *J. Phys. Chem.*, **95**, 9955–9960 (1991).

Kaneko, K. et al., "The Concentrated NO Dimer in Micropores at Room Temperature," *J. Chem. Phys.*, **87**, 776–777 (1987).

Kaneko, K. et al., "Characterization of iron oxide-dispersed activated carbon fibers with iron k-edge XANES and with water adsorption and fe k-edge XANES and EXAFS," *J. Chem. Soc. Faraday Trans. I*, **85**, 869–881 (1989).

Kaneko, K. et al., "Nitrogen Adsorption in Slit Pores at Ambient Temperatures: Comparison of Simulation and Experiment," *Langmuir*, **10**, 4606–4609 (1994).

Kaneko, K. et al., "Cluster-Mediated Water Adsorption on Carbon Nanopores," *Adsorption*, **5**, 7–13 (1999).

Kaneko, K. et al., "A Remarkable Elevation of Freezing Temperature of CCl_4 in Graphitic Micropores," *J. Phys. Chem.*, **103**, 7061–7063 (1999).

Kaneko, K., "Specific Intermolecular Structures of Gases Confined in Carbon Nanospace," *Carbon*, **38**, 287–303 (2000).

Kimura, et al., "Cluster-Associated Filling of Water in Hydrophobic Carbon Micropores," *J. Phys. Chem.*, **108**, 14043–14048 (2004).

Menon, V.C. and S. Komarneni, "Porous Adsorbents for Vehicular Natural Gas Storage: A Review," *J. Porouos Mater.*, **5**, 43–58 (1998).

Mowia, D. et al., "Adsorption of Water Vapor on Activated Carbon: A Brief Overview," *Chem. Phys. Carbon*, **28**, 229–262 (2004).

Murata, K. et al., "Adsorption Mechanism of Supercritical Hydrogen in Internal and Interstitial Nanospaces of Single Wall Carbon Nanohorn Assembly," *J. Phys. Chem. B.*, **106**, 11132–11138 (2002).

Nishi, Y. et al., "Ambient Temperature Reduction of NO to N_2 in Ru-Tailored Carbon Subnanospace," *J. Phys. Chem. B*, **101**, 1938–1939 (1997).

Ohba, T. et al., "Preformed Monolayer-Induced Filling of Molecules in Micropores," *Chem. Phys. Lett.*, **326**, 158–162 (2000).

Ohba et al., "N_2 Adsorption in an Internal Nanopore Space of Single Walled Carbon Nanohorn-GCMC Simulation and Experiment," *Nano Lett.*, **1**, 371–373 (2001).

Ohba et al., "Nanopore Characterization of GCMC-aided N_2 adsorption," *J. Phys. Chem.* To be submitted.

Ohba, T et al., "Affinity Transformation from Hydrophilicity to Hydrophobicity of Water Molecules on the Basis of Adsorption of Water in Graphitic Nanopores," *J. Amer. Chem. Soc.* **126**, 156–1562 (2004).

Ohkubo, T. et al., "Pore Width-Dependent Ordering of C_2H_5OH Molecules Confined in Graphitic Slit Nanospaces," *J. Phys. Chem. B*, **103**, 1859–1863 (1999).

Ohkubo, T. and K. Kaneko, "Oriented Structure of Alcohol Confined in Carbon Micropores with ERDF Analysis," *Colloid Surf.*, **A187–188**, 177–185 (2001).

Ohkubo, T. et al., "Restricted Hydration Structures of Rb and Br Ions Confined in Slit-Shaped Carbon Nanospaces," *J. Am. Chem. Soc.*, **124**, 11860–11861 (2002).

Ohkubo, T. et al., "Nanosolution as a New Turn of Nanoconfinement for Fluids," *Aust. J. Chem.* **56**, 1013–1016 (2003).

Ohkubo, T. et al., "Structural Anomalies of Rb and Br Ionic Nanosolutions in Hydrophobic Slit-Shaped Solid Space as Revealed by the EXAFS Technique," *J. Phys. Chem. B*, **107**, 13616–13622 (2003).

Oren, Y. and A. Soffer, "The Electrical Double Layer of Carbon and Graphite Electrodes," *J. Electroanal. Chem.*, **186**, 63–77 (1985).

Radhakrishnan, R. et al., "Freezing of Simple Fluids in Microporous Activated Carbon Fibers: Comparison of Simulation and Experiment," *J. Chem. Phys.*, **111**, 9058–9067 (1999).

Saito, R. et al., *Physical Properties of Carbon Nanotubes*, Imperial College Press, London 1998.

Suzuki, T. et al., "Quasi-Symmetry Structure of CCl_4 Molecular Assemblies in a Graphitic Nanopore," *Langmuir*, **15**, 5870–5875 (1999).

Tanahashi, et al., "Electrochemical Characterization of Activated Carbon Fiber Cloth Polarizable Electrode for Electric Double-Layer Capacitors," *J. Electrochem. Soc.*, **137**, 3052–3057 (1990).

Tanaka, H. et al., "Quantum Effects on Hydrogen Adsorption in Internal Nanospaces of Single-Wall Carbon Nanohorns," *J. Phys. Chem.*, in press.

Tanaka, H. et al., "Quantum Effect on Isotopic Adsorption of Hydrogen in Nanospaces of Single Wall Carbon Nanohorn," *J. Amer. Chem. Soc.*, to be submitted.

Tanaka, K., et al., *The Science and Technology of Carbon Nanotubes*, Elsevier, Amsterdam 1999.

Todoh, A. and K. Kaneko, "Effect of CO_2 on Magnetism of O_2 Confined in Graphitic Slit-Shaped Micropores," *Chem. Phys. Lett.*, **340**, 33–38 (2001).

Yang, C-M., et al., "Adsorption Behaviors of HiPco Single Walled Carbon Nanotube Aggregates for Alcohol Vapors," *J. Phys. Chem.*, *B* **106**, 8994–8999 (2002).